



Aalborg Universitet

AALBORG UNIVERSITY  
DENMARK

## Micropollutant Oxidation Studied by Quantum Chemical Computations

*Methodology and Applications to Thermodynamics, Kinetics, and Reaction Mechanisms*

Tentscher, Peter Rudolf; Lee, Minju; von Gunten, Urs

*Published in:*  
Accounts of Chemical Research

*DOI (link to publication from Publisher):*  
[10.1021/acs.accounts.8b00610](https://doi.org/10.1021/acs.accounts.8b00610)

*Publication date:*  
2019

*Document Version*  
Accepted author manuscript, peer reviewed version

[Link to publication from Aalborg University](#)

*Citation for published version (APA):*

Tentscher, P. R., Lee, M., & von Gunten, U. (2019). Micropollutant Oxidation Studied by Quantum Chemical Computations: Methodology and Applications to Thermodynamics, Kinetics, and Reaction Mechanisms. *Accounts of Chemical Research*, 52(3), 605-614. <https://doi.org/10.1021/acs.accounts.8b00610>

### General rights

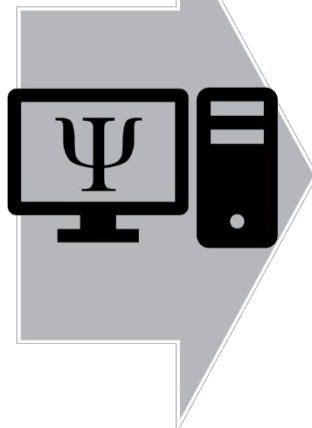
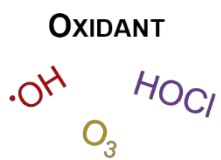
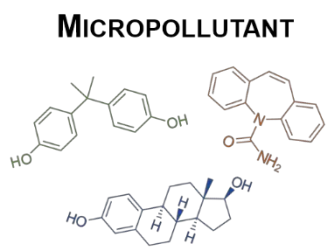
Copyright and moral rights for the publications made accessible in the public portal are retained by the authors and/or other copyright owners and it is a condition of accessing publications that users recognise and abide by the legal requirements associated with these rights.

- Users may download and print one copy of any publication from the public portal for the purpose of private study or research.
- You may not further distribute the material or use it for any profit-making activity or commercial gain
- You may freely distribute the URL identifying the publication in the public portal -

### Take down policy

If you believe that this document breaches copyright please contact us at [vbn@aub.aau.dk](mailto:vbn@aub.aau.dk) providing details, and we will remove access to the work immediately and investigate your claim.

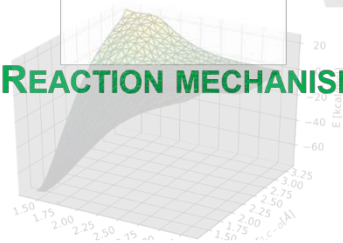




**REACTION KINETICS**

**THERMODYNAMICS**

**REACTION MECHANISMS**



16

## 17 **CONSPECTUS**

18 The abatement of organic micropollutants during oxidation processes has become an  
19 emerging issue for various urban water systems such as drinking water, wastewater  
20 and water reuse. Reaction kinetics and mechanisms play an important role in terms of  
21 efficiency of these processes and the formation of transformation products, which are  
22 controlled by functional groups in the micropollutants and the applied oxidants. So  
23 far, the kinetic and mechanistic information of the underlying reactions was obtained  
24 by experimental studies, additionally, predictive quantitative structure activity  
25 relationships (QSARs) were applied to determine reaction kinetics for the oxidation of  
26 emerging compounds. Since this experimental approach is very laborious and there  
27 are tens of thousands potential contaminants, alternative strategies need to be  
28 developed to predict the fate of micropollutants during oxidative water treatment. Due  
29 to significant developments in quantum chemical (QC) computations in recent years  
30 and increased computational capacity, QC-based methods have become an alternative  
31 or a supplement to the current experimental approach.

32

33 This article provides a critical assessment of the current state-of-the-art of QC-based  
34 methods for the assessment of oxidation of micropollutants. Starting from a given  
35 input structure, QC computations need to locate energetic minima on the potential  
36 energy surface (PES). Starting from these minima, useful thermodynamic and kinetic  
37 information can be estimated by different approaches: Experimentally determined  
38 reaction mechanisms can be validated by identification of transition structures in the  
39 PES, which can be obtained for addition reactions, heavy atom transfer ( $\text{Cl}^+$ ,  $\text{Br}^+$ ,  $\text{O}^+$ )  
40 and H-atom transfer (simultaneous proton and electron transfer) reactions. However,  
41 transition structures in the PES cannot be obtained for  $e^-$ -transfer reactions (SI, Text  
42 S8).

43 Second order rate constants  $k$  for the reactions of micropollutants with chemical  
44 oxidants can be obtained by *ab initio* calculations or by quantitative structure activity  
45 relationships (QSARs) with various QC descriptors. It has been demonstrated that  
46 second order rate constants from *ab initio* calculations are within factors 3-750 of the  
47 measured values, whereas LFER-based methods can achieve factors 2-4 compared to  
48 the experimental data. The orbital eigenvalue of the highest occupied molecular

49 orbital ( $E_{\text{HOMO}}$ ) is the most commonly used descriptor for LFER-based computations  
50 of  $k$ -values.

51 In combination with results from experimental studies, QC computations can also be  
52 applied to investigate reaction mechanisms for verification/understanding of oxidative  
53 mechanisms, calculation of branching ratios or regioselectivity, evaluation of the  
54 experimental product distribution and assessment of substitution effects. Furthermore,  
55 other important physical-chemical constants such as unknown equilibria for species,  
56 which are not measurable due to low concentrations or  $\text{p}K_{\text{a}}$  values of reactive  
57 transient species can be estimated. With further development of QC-based methods, it  
58 will become possible to implement kinetic and mechanistic information from such  
59 computations in *in silico* models to predict oxidative transformation of  
60 micropollutants. Such predictions can then be complemented by tailored experimental  
61 studies to confirm/falsify the computations.

62

## 63 **INTRODUCTION**

### 64 ***Reactions of chemical oxidants with micropollutants***

65 Chemical oxidants (e.g., chlorine, ozone, chlorine dioxide, etc.) have been applied in  
66 water treatment since more than a century, first for disinfection and later for  
67 micropollutant abatement.<sup>1</sup> Chemical oxidants react mainly with water matrix  
68 components such as the dissolved organic matter (DOM),<sup>1</sup> however in this article, we  
69 will focus on the oxidative abatement of micropollutants, which has become a major  
70 issue for drinking water, in water reuse systems, and enhanced municipal wastewater  
71 treatment systems.<sup>1</sup> Typically, oxidation does not lead to a complete mineralization of  
72 target micropollutants but to transformation products with initially similar structures  
73 as the parent compounds.<sup>1</sup> Biologically active target compounds are inactivated by  
74 these relatively minor changes in their molecular structures.<sup>1</sup> For extended oxidation  
75 of micropollutants low molecular weight compounds will be formed, with limited or  
76 no structural similarities to the target compounds, which may be of toxicological  
77 concern.<sup>1</sup>

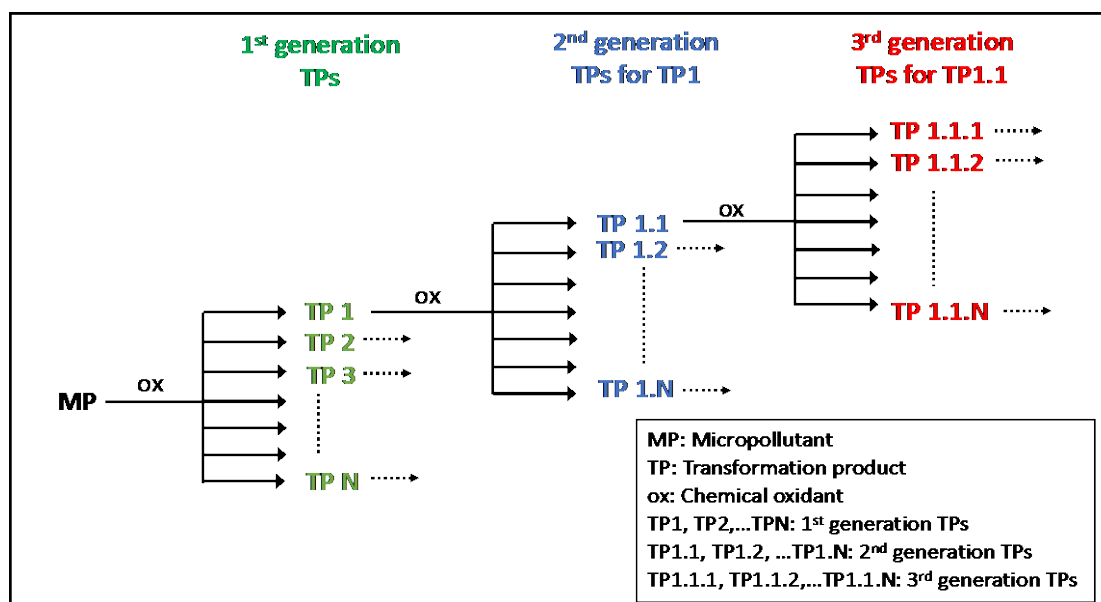
### 78 ***Assessment of oxidation processes***

79 So far, the efficiency of oxidation processes has been mainly assessed experimentally.  
80 There is a large body of information on the kinetics and mechanisms of the reactions  
81 of functional groups and micropollutants with chemical oxidants.<sup>1</sup> However, a purely

82 experimental approach for kinetic and mechanistic studies is labor-intensive and time  
 83 consuming. If only a fraction of the about 100'000 commercially available chemicals  
 84 can be found in water treatment systems (especially wastewater and water reuse), it  
 85 will be almost impossible to determine reaction kinetics, mechanisms and  
 86 transformation products experimentally (Figure 1).<sup>1</sup>

87

88



89

90 Figure 1. Reactions of chemical oxidants with synthetic organic compounds (MPs). A  
 91 simplified reaction scheme illustrates the complexity for the formation of TPs.

92 Dashed arrows: Analogous reactions to TP1, TP1.1 and TP1.1.1 (not shown).

93

94 Rather, a focus on fundamental kinetic and mechanistic aspects with the main  
 95 oxidant-reactive functional groups is promising. This knowledge can then be  
 96 extrapolated to realistic systems to assess transformation product formation based on  
 97 the knowledge of functional groups of the reaction targets.<sup>1</sup>

98

99 ***Predictive methods for oxidation kinetics and mechanisms***

100 It is evident that prognostic tools are needed to estimate kinetic parameters and  
 101 determine mechanisms for oxidant-target compound reactions for the huge number  
 102 compounds.

103 *Reaction kinetics*

104 Second-order rate constants for the reactions of organic compounds with oxidants  
105 such as hydroxyl radical, ozone, chlorine, bromine, chlorine dioxide, ferrate(VI) and  
106 permanganate have been experimentally determined and compiled.<sup>2-9</sup> Based on this  
107 information, second-order rate constants for the reactions of emerging compounds  
108 with oxidants can be estimated by quantitative structure activity relationships  
109 (QSAR). This approach has been successfully applied for activated aromatic  
110 compounds, olefins and amines for the oxidants ozone, chlorine, chlorine dioxide and  
111 ferrate(VI) with Hammett and Taft sigma coefficients.<sup>10</sup> Overall, predicted second-  
112 order rate constants within a factor of 1/3-3 of the measured values can be obtained,  
113 similar to the margin of different experimental studies. However, for complex  
114 chemical structures, Hammett or Taft coefficients are sometimes difficult to obtain.<sup>10</sup>  
115 Furthermore, second-order rate constants for the reactions of hydroxyl radical with  
116 organic compounds have been estimated by the group contribution method.<sup>11</sup> The  
117 advent of modern quantum chemical (QC) methodologies (e.g., density functional  
118 theory, DFT) and the high-performance computing provided an affordable means for  
119 theoretical investigations on oxidative reactions. Therefore, an alternative for  
120 estimating second-order rate constants is based on QC computations (see below).<sup>12</sup>  
121 This approach has the advantage that it is independent of Hammett or Taft sigma  
122 values, which are not available for all chemical structures.

### 123 *Reaction mechanisms*

124 Transformation pathways during oxidative treatment of micropollutants can be  
125 determined by labor-intensive experiments by analyzing transformation products by a  
126 suite of analytical tools.<sup>1</sup> Such information has been applied to build computer-  
127 assisted pathway prediction systems based on reaction rules for ozone and hydroxyl  
128 radical.<sup>13-14</sup> For other oxidants applied in water treatment (e.g., chlorine, chlorine  
129 dioxide, permanganate, etc.), no comprehensive compilations of mechanistic  
130 information are available and it is more difficult to predict reaction products.  
131 Generally, the uncertainty of predictions increases with the extent of transformation  
132 of the target compound, i.e., from the first-generation products to higher generation  
133 products (Fig. 1). Based on the reaction mechanisms provided in literature, it is often  
134 difficult to judge the likelihood of specific reactions among multiple pathways.  
135 It has been demonstrated, that QC computations can complement or even substitute  
136 experimental kinetic and mechanistic studies on the oxidation of organic  
137 compounds.<sup>15-16</sup> The goals of this paper are to (i) discuss the state-of-the-art of QC

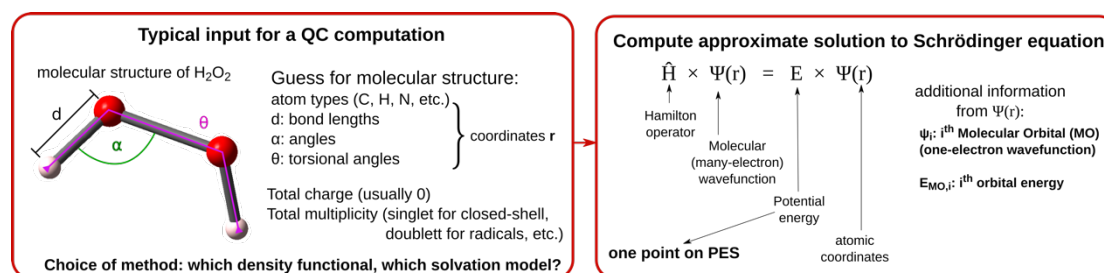
138 computations for oxidative processes, (ii) give examples and a critical evaluation of  
139 the work that has been performed in this field, and (iii) assess the practical  
140 implications of this approach.

# 141 QUANTUM CHEMICAL COMPUTATIONS: STATE-OF-THE-ART

## 142 General considerations

143 QC computations<sup>17</sup> simulate isolated molecules or complexes, as opposed to a  
144 solution containing molecules in high numbers. A typical input file and output is  
145 exemplified in Figure 2.

146

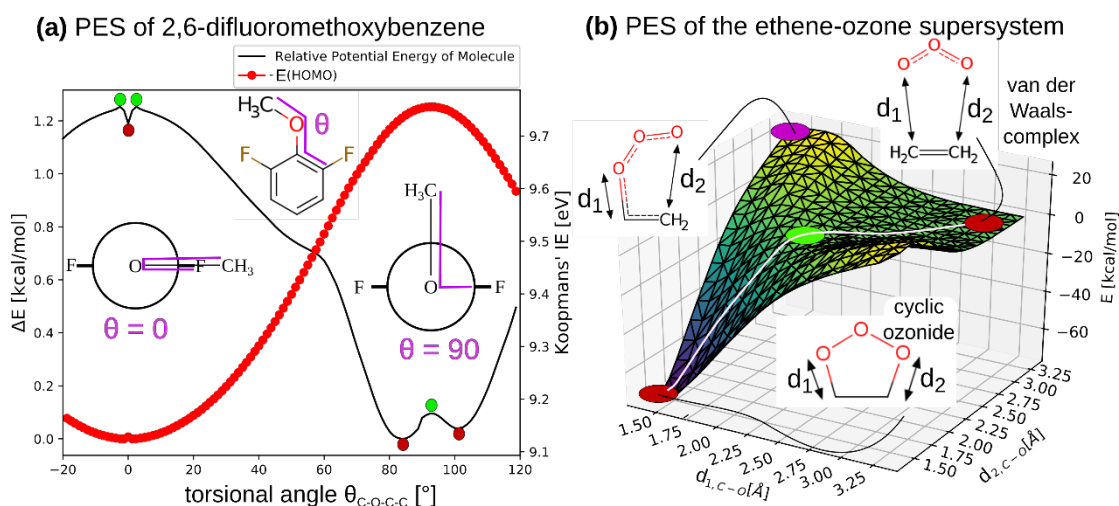


148 Figure 2: Required input for a QC computation and resulting information.

149

150 The approximate solution of the time-independent electronic Schrödinger equation  
151 depends on the atomic coordinates  $r$  (bond lengths, angles, and torsional angles) as  
152 parameters only (Born-Oppenheimer approximation) and yields the potential energy  $E$   
153 for a given set of coordinates (Figure 2). These  $3N-6$  degrees of freedom ( $N$ =number  
154 of atoms) define a potential energy surface (PES, Figure 3). The reactant and product  
155 species of a reaction are defined by differences in  $r$  only, and the number of atoms has  
156 to remain balanced for calculation of energy differences. From a given input structure,  
157 a computer program will find the closest energetic minima (stationary structures) on  
158 the PES, corresponding to observable chemical species. Based on this, further  
159 analyses can lead to information on kinetics, thermodynamics, and reaction  
160 mechanisms, which is elucidated in Figure 4.

161



162

163 Figure 3: The 3N-6-dimensional PES can be collapsed to one or two dimensions by  
 164 systematically varying *one or two coordinates*, and optimizing the rest of the system.

165 (a) *Dihedral angle* of the  $H_3C-O-C-CF$  torsion of 2,6-difluoromethoxybenzene (b)

166 *Two  $r_{C-O}$  distances* of the  $O_3$ -ethene supersystem. Minima on the PES are marked in

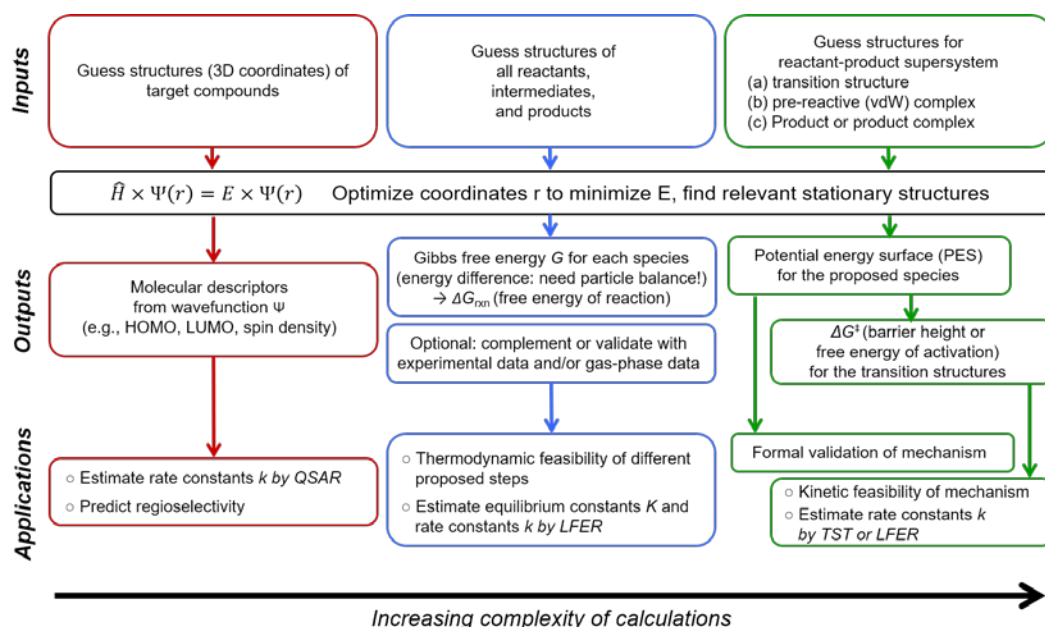
167 red, the transition structure connecting the minima in green. (b) also shows the

168 potential structure for a monodentate adduct (purple) and the minimum energy

169 path/“reaction coordinate” connecting reactants and products in white (computational

170 details: Supporting Information(SI) Text S7).

171



172

173 Figure 4: Calculation schemes with various complexities for obtaining the relevant

174 QC parameters of different applications as discussed in the manuscript. LFER: Linear

175 free energy relationship, TST: Transition state theory

176

177 **Evaluation of  $\Delta G_{\text{rxn}}$  (thermodynamic feasibility and equilibria)**

178 Gibbs free energy ( $G$  or free energy hereafter) can be used to evaluate thermodynamic  
179 feasibility or equilibria of a reaction (Figure 4, middle). This is implemented  
180 following the thermodynamic cycle summarized in eq. (1), yielding the aqueous free  
181 energy of reaction  $\Delta G_{\text{rxn}}$ .

182 
$$\Delta G_{\text{rxn}} = \sum G_{\text{products,gas}} + \sum \Delta G_{\text{products,solv}} - \sum G_{\text{reactants,gas}} - \sum \Delta G_{\text{reactants,solv}} \quad (1)$$

183 Only structures of individual species need to be provided, and can usually be easily  
184 proposed. Moreover, the computation can be divided into a gas phase component and  
185 a free energy of solvation  $\Delta G_{\text{solv}}$ ,<sup>18</sup> allowing for the use of highly accurate methods  
186 (e.g., coupled cluster<sup>19</sup>) or experimental values for gas phase  $\Delta G_{\text{rxn}}$ . The accuracy of  
187 such calculations strongly depends on the model chemistry used for both the gas  
188 phase and the solvation parts.

189 For gas phase energetics, the “gold standard” CCSD(T) method<sup>19</sup> (SI, Text S1) can  
190 achieve an accuracy of 1 kcal/mol ( $\cong$  experimental accuracy) for many problems of  
191 organic chemistry, and should be used whenever affordable. Table 1 illustrates that  
192 the uncertainty in thermodynamic properties stems primarily from the solvation  
193 model, especially for ionic compounds. However, for some of the primary and  
194 secondary oxidants bearing “multireference character” (including  $\text{Cl}_2\text{O}$ ,<sup>20</sup>  $\text{ClO}_2$ ,<sup>20</sup>  
195  $\text{O}_3$ ,<sup>21</sup>  $\text{O}_3^-$ , and  $^1\text{O}_2$ ),<sup>21</sup> and any singlet diradical intermediates (SI, Text S9), gas phase  
196 results alone may already be equally uncertain. For example, free energy calculations  
197 involving  $\text{O}_3$  as a reactant suffer from a systematic error in  $\Delta G_{\text{rxn}}$  of  $\sim 4$  kcal/mol in the  
198 gas phase electronic energy component when computed by CCSD(T), and even worse  
199 with contemporary DFT methods.<sup>21</sup> More sophisticated methods are necessary to  
200 reach 1 kcal/mol accuracy,<sup>19, 21</sup> which are not affordable for any target compounds of  
201 interest. Careful method evaluation using smaller model compounds can be used to  
202 select methods with reasonable results for real systems (SI, Text S1 for a discussion  
203 of accuracy versus computer time).

204 In many difficult cases, lacking thermodynamic data can be compiled from  
205 experimental data. Gas phase reaction energies, but also experimental  $\text{p}K_{\text{a}}$  values,  
206 redox potentials, or other equilibrium constants (linked to free energy differences  
207 through  $\log(K) = \Delta G/RT$ ) can be used in thermodynamic cycles to estimate desired  
208 free energy differences or free energies of solvation needed for aqueous phase  
209 calculations. This requires that the other components of the thermodynamic cycle are

210 computed close to experimental accuracy. Table 1 provides some examples of  
211 achievable accuracies for such thermochemical simulations.

212

213 Table 1: Typically achievable average accuracies for thermodynamic parameters from

214 QC computations.<sup>a</sup>

<b>Thermodynamic parameter</b>	<b>Accuracy</b>
$\Delta G_{\text{rxn}}$ (gas phase)	CCSD(T)/composite: ~1-2 kcal/mol <sup>19</sup> (~4 kcal/mol) <sup>d21</sup> DFT: 2-4 kcal/mol <sup>24</sup>
$\Delta G_{\text{solv}}$ (neutral species)	Implicit solvation: <sup>d</sup> 1-2 kcal/mol <sup>25</sup>
$\Delta G_{\text{solv}}$ (ionic species)	Implicit solvation: <sup>d</sup> 3-7 kcal/mol <sup>25</sup>
$\text{p}K_{\text{a}}$	Implicit solvation only: <sup>d</sup> ~6 pH units <sup>26</sup> Implicit solvation with some explicit water molecules: <sup>e</sup> ~1 pH unit <sup>26</sup>
IE (gas) <sup>b</sup>	CCSD(T)/composite: ~1-2 kcal/mol <sup>27-28</sup> DFT: ~3-5 kcal/mol <sup>28</sup>
$\Delta G^{\text{oc}}$	Implicit solvation: <sup>d</sup> ~0.3 V (~7 kcal/mol) <sup>29</sup> Explicit solvation: <sup>d</sup> ~0.2 V (~4 kcal/mol) <sup>30</sup>

215 <sup>a</sup>Results should be compared to experimental data of similar systems (e.g.,  
216 equilibrium constants of halogen oxides<sup>22</sup>), or can be correlated to experimental data  
217 of a congeneric series (e.g., one-electron oxidation potentials of anilines<sup>23</sup> see SI, Text  
218 S1)

219 <sup>b</sup>gas phase adiabatic ionization energy

220 <sup>c</sup>half-cell standard reduction potential

221 <sup>d</sup>reduced accuracy for multi-reference species

222 <sup>e</sup>SI, Text S2 for details on implicit and explicit solvation

223

## 224 **Computational validation of proposed reaction mechanisms**

225 For further mechanistic validation, stationary structures on the PES of combined  
226 reactants need to be identified: (a) The pre-reactive complex of the reactants, (b) the  
227 product (complex), and (c) a transition structure (first order saddle point on the PES)  
228 connecting the reactant with the product side through a minimum energy path (Figure  
229 3b).

230 This is possible if the minimum energy path can be easily expressed by atomic  
231 coordinates (e.g., by one or two interatomic distances). However, oxidants react by  
232 different mechanisms including electron transfer (ET) (Table 2) or variations thereof,  
233 where transition structures cannot be identified like this (Table 3).

234 When describing bond formation/cleavage, common QC methods suffer from a poor  
235 description of largely elongated bonds,<sup>17, 19</sup> resulting in inaccurate energetics, and in  
236 the worst case in qualitative differences in the PES described by different methods  
237 (SI, Text S3). Such extreme problems should only arise when a molecular diradical is  
238 involved.

239 Frequently, the initial reaction of an oxidant with a target compound will not lead to  
240 the experimentally observed “primary” product, but to metastable intermediate(s) that  
241 cannot be observed experimentally (Figure 1). However, only computing a complete  
242 pathway from reactant to product can support a proposed reaction mechanism, which  
243 can be quite laborious. Computed  $\Delta G^\ddagger$  (barrier height or free energy of activation) can  
244 be used as an additional criterion concerning the kinetic feasibility of a computed  
245 mechanism, and can provide some insight into the kinetic control of the formation of  
246 possible products.

247

248 Table 2: Common oxidants in water treatment and the corresponding reaction  
249 mechanisms

Oxidant	Proposed reaction mechanisms
O <sub>3</sub>	Addition, H-atom transfer, e <sup>-</sup> -transfer, O-transfer
HOCl	Cl <sup>+</sup> -transfer, e <sup>-</sup> -transfer
Cl <sub>2</sub> O	Cl <sup>+</sup> -transfer, e <sup>-</sup> -transfer
HOBr	Br <sup>+</sup> -transfer, e <sup>-</sup> -transfer
ClO <sub>2</sub>	e <sup>-</sup> -transfer
<sup>•</sup> OH	Addition, H-atom transfer, e <sup>-</sup> -transfer
Fe(VI)	e <sup>-</sup> -transfer, addition, oxygen-transfer
<sup>1</sup> O <sub>2</sub>	Addition

250

251 Table 3: Feasibility of PES computations to identify transition structures

Mechanism	PES / minimum energy path
Addition	Yes
(Heavy) atom transfer ( $\text{Cl}^+$ , $\text{Br}^+$ , $\text{O}^\bullet$ )	Yes
H-atom transfer	Yes (if proton and electron are transferred simultaneously)
$e^-$ -transfer	No (including proton-coupled electron transfer and similar)

252

253

254 **Kinetics of reactions: Second-order rate constants  $k$** 

255 Kinetic experiments for a bimolecular reaction between a target compound (Red) and  
 256 an oxidant (Ox) measure an apparent second-order rate constant  $k_{app}$  ( $\text{M}^{-1}\text{s}^{-1}$ , typically  
 257 determined at 298K and 1atm), which is a lump sum of different microscopic  
 258 reactivities (eq. 2):

$$259 \quad -\frac{d}{dt}[\text{Red}] = k_{app}[\text{Red}_{tot}][\text{Ox}_{tot}] = \sum_i^n \sum_j^m \sum_l^o k_{ijl}[\text{Red}_i][\text{Ox}_j] \quad (2)$$

260 where “tot” signifies total concentrations. The triple summation corresponds to ( $i$ )  
 261 speciation in the target compound, ( $j$ ) speciation in the oxidant, and ( $l$ ) different  
 262 reaction channels for a species-specific reaction. Therefore,  $k_{ijl}$  is a microscopic rate  
 263 constant specific to a certain  $i$ - $j$  species pair and a channel  $l$ . Simulated rate constants  
 264 are computed from a specific molecular geometry, thus correspond to  $k_{ij}$  (species-  
 265 specific) or  $k_{ijl}$  (channel-specific). In experiments, in contrast, pH-dependent  
 266 speciation for the target compound and oxidant can be typically deconvoluted with  
 267 the  $\text{p}K_a$ , while other species-specific (e.g., conformers) and channel-specific  $k$  remain  
 268 indistinguishable (SI, Text S4). Therefore, a careful comparison between theoretical  
 269 and experimental  $k$  is required for verification.

270

271 *ab initio* calculations of  $k$  by Transition State Theory (TST)

272 Identified transition structures allow the calculation of  $\Delta G^\ddagger$  (Figure 4, right), which is  
 273 linked to the rate constant through TST, using the Eyring-Polanyi equation (Table 4).  
 274 Calculation of absolute microscopic rate constants requires detailed knowledge of the  
 275 reaction mechanism(s)/transition structures, along with further corrections to the rate

276 expression.<sup>31</sup> There are several limitations to this approach: (a) Calculations including  
 277 “problematic” oxidants such as O<sub>3</sub> (and probably also ClO<sub>2</sub>, Cl<sub>2</sub>O, CO<sub>3</sub><sup>•-</sup>) suffer from  
 278 shortcomings of the used electronic structure method. (b) Ionic transition structures  
 279 can be significantly stabilized by water molecules (which are lacking from the usually  
 280 employed implicit solvation models) or may be catalyzed by proton transfer to and  
 281 from neighboring water molecules, (c) limitations of the Eyring-Polanyi equation or  
 282 similar approaches (e.g., the transmission coefficient is unknown for solution-phase  
 283 reactions, and well-defined quasi-equilibria are assumed) (SI, Text S5). Estimation of  
 284  $\log(k)$  close to experimental accuracy ( $\sim 1 \log(k)$ ) would typically require an accuracy  
 285 in  $\Delta G^\ddagger$  of  $< 2$  kcal/mol, which can never be warranted (Table 1). If computed and  
 286 experimental  $\log(k)$  differ by  $> 2$ , this could still be due to the technical limitations of  
 287 the simulation, or the rate-determining step of the reaction was not properly identified  
 288 on the PES.

289 For ET reactions, transition structures are not easily identified, and rate expressions  
 290 such as the Marcus or Sandros-Boltzmann equation are often used (Table 4). They  
 291 express  $\Delta G^\ddagger$  as a free energy difference and a fitting parameter (assumed to be  
 292 constant for the studied reactions). Computational estimation of redox properties is  
 293 too inaccurate<sup>27, 29-30</sup> to calculate absolute rate constants.

294

295 Table 4: Simplified rate constant expressions relevant to nucleophile-electrophile  
 296 interactions (SI, Text S5).

297

Eyring-Polanyi	Marcus	Sandros-Boltzmann	Klopman-Salem
$\log(k) \propto -\frac{\Delta G^\ddagger}{RT}$	$\log(k) \propto -\frac{(\lambda + \Delta G^\circ)^2}{4\lambda k_B T}$	$\log(k) \propto \frac{\Delta G + s}{RT}$	$\log(k) \propto \frac{\beta_{HOMO-LUMO}^2}{E_{HOMO,nuc} - E_{LUMO,elec}}$
$\Delta G^\ddagger$ : free energy of activation	$\Delta G^\circ$ : difference in electrode potentials (free energy of electron transfer) $\lambda$ : reorganization energy (fitting parameter in	$\Delta G$ : free energy of reaction $s$ : fitting parameter to a set of experimental rate constants	$E_{HOMO}$ : HOMO <sup>a</sup> energy on nucleophile $E_{LUMO}$ : LUMO <sup>b</sup> energy on electrophile $\beta$ : HOMO-LUMO resonance integral

	experimental work)		
	$k_B$ : Boltzmann constant		

298 <sup>a</sup>HOMO: Highest occupied molecular orbital; <sup>b</sup>LUMO: Lowest unoccupied  
 299 molecular orbital

300

301 *k* estimation from molecular descriptors *D*

302 A more common, pragmatic approach to estimate *k* is by regression models (e.g.,  
 303 QSAR) (eq. 3):

$$304 \log(k_a) = \sum c_b \times D_{a,b} + C \quad (3)$$

305 where *k* is the second-order rate constant for the reaction between a target compound  
 306 *a* and a specific oxidant,  $D_{a,b}$  is the  $b^{\text{th}}$  descriptor derived from the molecular structure  
 307 of the target compound *a*,  $c_b$  are coefficients fitted to experimental *k* values of a  
 308 specific oxidant, and *C* is a constant. A comparison to common rate expressions  
 309 (Table 4) shows that *D* has to be proportional to  $\Delta G^\ddagger$  or its electrochemical  
 310 formulations, irrespective of the reaction mechanism.

311

312 *Conceptual scope and limitations of QC descriptors*

313 Among different descriptors, the orbital eigenvalue of the highest occupied molecular  
 314 orbital ( $E_{\text{HOMO}}$ , contained in  $\Psi$ ) of the target compound is the most commonly used.  
 315 This is not surprising, as it relates to all relevant rate expressions (Table 4):

316 (i) The Klopman-Salem equation describes the ease of bond-making between a  
 317 nucleophile (target compound) and an electrophile (oxidant) by a donor-acceptor  
 318 orbital interaction. This electron flux from the HOMO of the nucleophile to the  
 319 LUMO of the electrophile is most favorable when this HOMO-LUMO energy gap is  
 320 small.

321 (ii) The Marcus and Sandros-Boltzmann equations relate the rate constant of an  
 322 electron transfer reaction to the free energy change and a fitting parameter ( $\lambda$  or *s*).  
 323 The free energy change is caused by removing an electron from the target compound,  
 324 and transferring it to the oxidant, corresponding to the adiabatic ionization energies  
 325 (IE/oxidation potential) and electron affinities (EA/reduction potential) of the  
 326 reactants (eq. 4):

$$327 \Delta G^\circ = \text{IE}(\text{reductant}) + \text{EA}(\text{oxidant}) \quad (4)$$

328 Koopmans' theorem<sup>32-33</sup> states that the  $-E_{\text{HOMO}} \cong \text{IE}$  of a molecule, and  $-E_{\text{LUMO}} \cong \text{EA}$ ,  
329 which are however vertical (non-adiabatic) quantities. In the Marcus theory, the  
330 difference between vertical and adiabatic electron transfer energies is the  
331 reorganization energy  $\lambda$ .

332 When considering a regression model of a single oxidant, its reduction potential or  
333 EA remain constant, and thus any form of computed IE of the target compound can be  
334 linked to electron transfer and/or bond-making reactions. Orbital energies have also  
335 been used as descriptors for H-atom transfer reactions, and these can be expected to  
336 be strongly correlated for a congeneric series (e.g., "phenols").<sup>34</sup> Thus, descriptors  
337 related to the IE are not mechanism-specific.

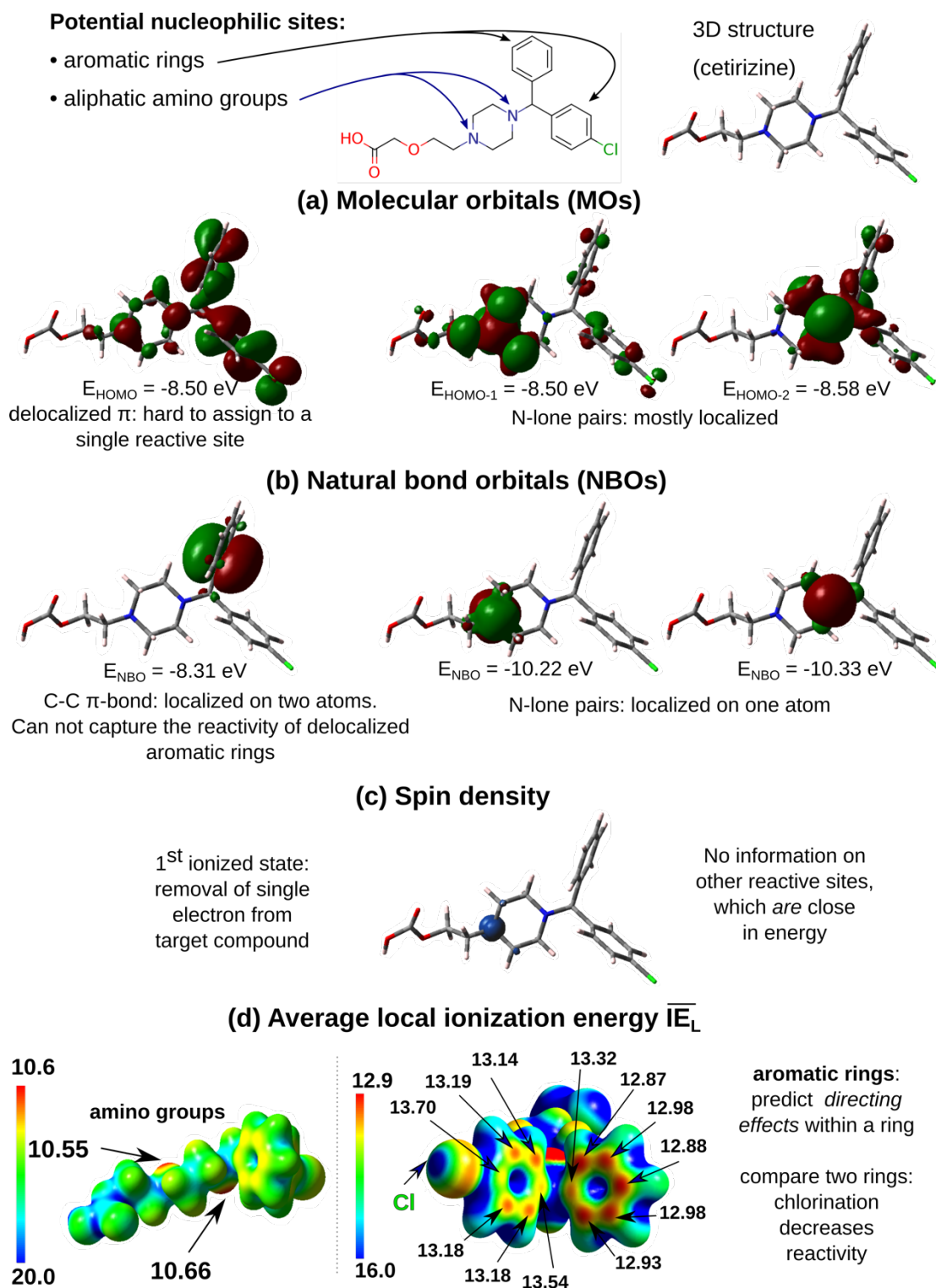
338 There are several caveats noteworthy when estimating  $k$  with QC descriptors.  
339 Orbital/ionization energies cannot account for steric effects, and imply that the rate-  
340 determining step of the reaction is the initial attack of the oxidant on the target  
341 compound. Moreover, when considering all relevant species according to eq. 2, in  
342 contrast to protonation state, conformational speciation remains undetected  
343 experimentally, but can have a large impact on calculated rate constants. Figure 3a  
344 shows the evolution of  $-E_{\text{HOMO}}$  with the torsional angle of the methoxy group of 2,6-  
345 difluoromethoxybenzene. The competition between mesomeric effects and steric  
346 hinderance leads to two minima of PES that are only  $\sim 1.5$  kcal/mol apart. However,  
347 the change in  $-E_{\text{HOMO}}$  is 8-fold (12 kcal/mol). Similar effects can be expected  
348 whenever a torsion is associated with the disruption of mesomeric effects.  
349 Consequently, algorithms that automatically generate a single guess structure for a  
350 molecule have to be used cautiously (different conformations may need to be  
351 considered when necessary).

352 Besides speciation, different reaction channels can contribute to the observed  
353 reactivity of two well-defined species ( $k_{ij}$  vs.  $k_{ji}$ ). This can refer to different  
354 mechanisms (e.g., ET vs.  $\text{Cl}^+$ -transfer, Table 2), but also a reaction at different sites  
355 within an organic molecule. The used descriptors (IEs, orbital energies, bond  
356 dissociation energies) are usually not mechanism-specific enough to distinguish  
357 reaction channels. However, regioselectivity (different reactive sites) can be  
358 described.  $\Psi$  contains descriptors to predict the likely sites of oxidation reactions in  
359 target compounds. Examples beyond MOs (natural bond orbitals,<sup>35</sup> the average local  
360 ionization energy  $\text{IE}_L$ ,<sup>36</sup> and the spin density of an oxidized target compound) are

361 given in Figure 5. Additionally, calculated bond dissociation energies (X-H, X=C, O,  
 362 N, S, not shown) can reveal the most reactive sites for H-abstraction.

363

364



365

366 Figure 5: Insight into regioselectivity of cetirizine (SI, Text S6 for details). (a) MOs

367 are often delocalized over several reactive sites, (b) NBOs are perfectly localized on

368 one or two atoms, but fail to capture delocalization effects, (c) indicates the location

369 of the unpaired electron in a radical, (d) is a Koopmans-type ionization energy  
370 projected onto a surface. Descriptors (a)-(d) predict a higher reactivity of the left  
371 amino group.  
372  
373

374 **APPLICATION OF QUANTUM CHEMICAL COMPUTATIONS FOR**  
 375 **KINETIC AND MECHANISTIC OXIDATION STUDIES**

376 **Reaction kinetics**

377 QSAR models using QC descriptors have been proposed for several oxidants (Table  
 378 5).

379

380 Table 5: Examples of QSAR models for the determination of second-order rate  
 381 constants that use QC descriptors.

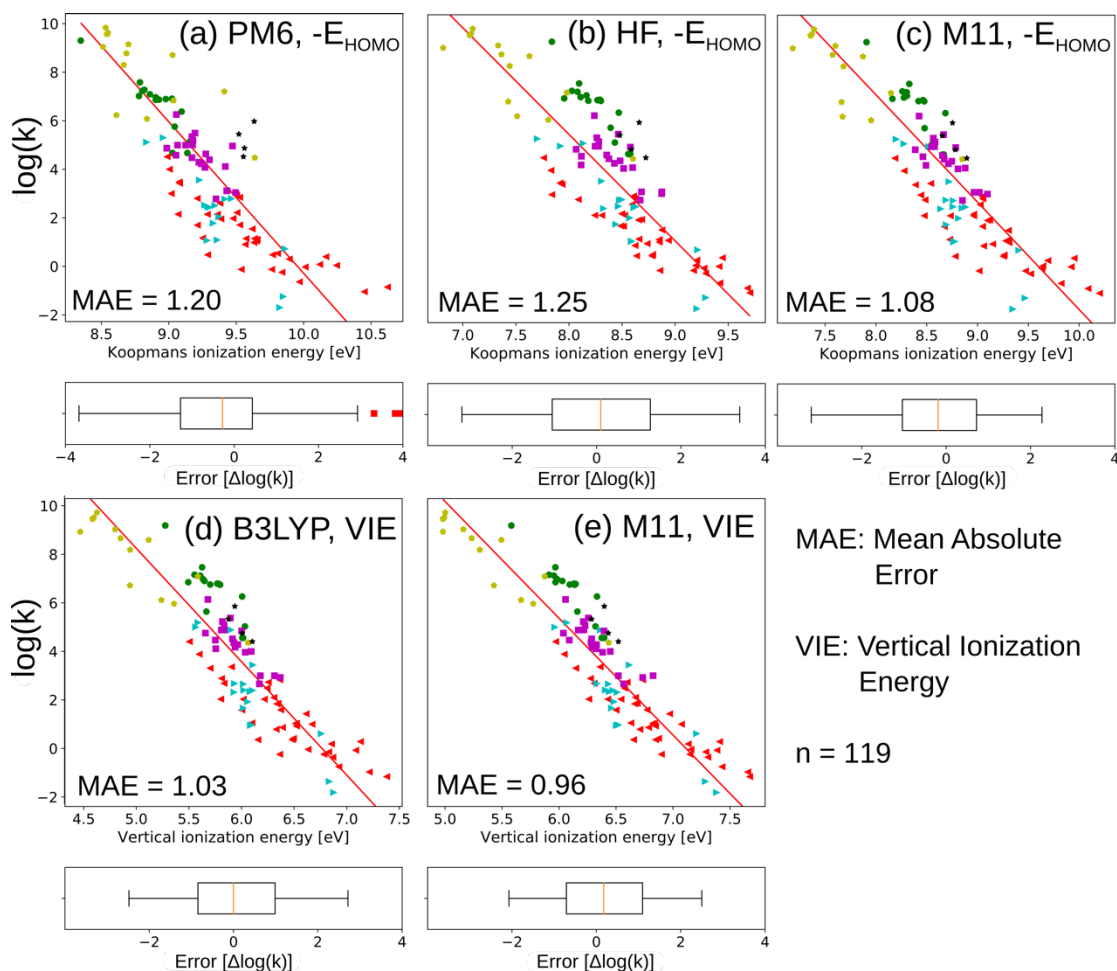
Oxidant	Target compounds	Descriptors	Rate constants
O <sub>3</sub>	aromatics <sup>12, 37</sup>	$E_{\text{HOMO}}$	$k_{ij}$
O <sub>3</sub>	olefins and amines, <sup>12</sup>	$E_{\text{NBO}}$	$k_{ij}$
O <sub>3</sub>	phenols <sup>38</sup>	VIE <sup>a</sup>	$k_{ij}$
O <sub>3</sub>	aromatics <sup>37</sup>	$\Delta G$ of adduct formation	$k_{ij}$
HO <sub>2</sub> <sup>•</sup> /O <sub>2</sub> <sup>-</sup>	various <sup>39</sup>	$E_{\text{HOMO}}/E_{\text{LUMO}}$	$k_{\text{app}}$
•OH	various <sup>40</sup>	$E_{\text{HOMO}}$	$k_{ij}$
•OH	various <sup>41-42</sup>	$\Delta G^{\ddagger}$ (LFER) <sup>b</sup>	$k_{ijl}$
<sup>1</sup> O <sub>2</sub>	olefins, aromatics, amines <sup>43</sup>	$E_{\text{HOMO}}$	$k_{\text{app}}$
<sup>1</sup> O <sub>2</sub>	phenols <sup>44</sup>	$\Delta G^{o c}$	$k_{ij}$
Carbonate radical	phenols, N-containing compounds <sup>44-45</sup>	$\Delta G^{o c}$	$k_{ij}$
Carbon-, chlorine- and oxygen-derived radicals	various inorganic species or disproportionation <sup>42, 46</sup>	$\Delta G^{\ddagger}$ (LFER) <sup>b</sup>	$k_{ijl}$

382 <sup>a</sup>VIE: Vertical ionization energy, <sup>b</sup>LFER: Linear Free Energy Relationship, <sup>c</sup>half-cell  
 383 standard reduction potential

384

385 Most of the proposed correlation models used experimental  $k_{ij}$  (protonation-state  
 386 specific), which collectively include all reaction channels.  $E_{\text{HOMO}}$  and  $E_{\text{NBO}}$  were

387 shown to be strongly correlated with the corresponding Hammett or Taft constants  
388 from the QSAR approach,<sup>12</sup> wherefore these descriptors are regarded as proxies  
389 reflecting the electron-donating/withdrawing effects of substituents on a reaction  
390 center. Ideally, the two types of descriptors should be mutually replaceable. QC  
391 descriptors yield sometimes results inferior to Hammett/Taft constants, which we  
392 ascribe partly to shortcomings in the electronic structure methods used to compute  
393 these descriptors. As  $-E_{\text{HOMO}}$  can be interpreted as an IE, differing quality of both  
394 descriptors can be expected from different methods, which is exemplified in Figure 6.  
395 Systematic errors may cancel within a group of congeneric target compounds, but  
396 more general models benefit from using methods that produce somewhat realistic  
397 ionization/orbital energies.<sup>33</sup> The same argument holds for thermodynamic descriptors  
398 such as bond dissociation energies or product formation energies. When considering  
399 congeneric classes of compounds, QSAR-predicted rate constants agree with  
400 experimental  $k_{ij}$  within a factor of 2-4.<sup>12</sup> However, the scope of such QSAR models is  
401 limited by the structures comprised in the experimental training data set.  
402 As an alternative to QSAR, absolute  $k$  computed from  $\Delta G^\ddagger$  by TST were within a  
403 factor of 3-750 from experimental values, depending on the oxidants, reaction types  
404 and models employed.<sup>12, 31,41, 47</sup>  
405



406

407

408 Figure 6: Univariate QSAR models for the  $\log(k)$  for the reactions between ozone and  
 409 aromatic compounds. Descriptors are  $E_{\text{HOMO}}$  calculated by (a) the semi-empirical  
 410 PM6 model, (b) the Hartree-Fock model, (c) the long-range corrected M11 density  
 411 functional, (d) and (e) explicitly calculated VIE using B3LYP and the generally more  
 412 accurate M11 functional (SI, Text S7).

413

#### 414 Reaction mechanisms and thermodynamic properties

415 Mechanistic insights allow (qualitative) conclusions on the types of compounds  
 416 undergoing a studied type of reaction. QC data provide information on what types of  
 417 intermediates can be formed, and if they are connected on the PES. This knowledge  
 418 can be used to determine the likelihood of the formation/type of transformation  
 419 products (Table 6). Reaction mechanisms often involve equilibria, which can be  
 420 estimated based on QC free energy calculations (Table 7).

421

422 Table 6: Illustrative examples of QC studies of oxidative reaction mechanisms

Reaction	Calculation type(s)	Gained information
<i>N,N</i> -dimethylsulfamide + O <sub>3</sub> <sup>47</sup>	$\Delta G/\Delta G^\ddagger$	Verification/understanding of Br <sup>-</sup> -catalyzed mechanism
Acetone + $\cdot\text{OH}$ <sup>48</sup>	$\Delta G/\Delta G^\ddagger/k$ of 88 possible elementary reactions from reactants to experimentally observed products	Comparison of theoretically simulated time-dependent concentration profiles of the target substance and oxidation products with experimental observations
Ratinidine + mono-/dichloramine <sup>49</sup>	$\Delta G/\Delta G^\ddagger$	Proposition of nitric oxide as reactive nitrosating agent (refuted by experiment) <sup>50</sup>
<i>p</i> -substituted phenols + O <sub>3</sub> <sup>38</sup>	$\Delta G/\Delta G^\ddagger$ of reactions following the initial addition of O <sub>3</sub>	Qualitative attribution of observed products to substituent-specific reaction mechanisms
Ibuprofen + $\cdot\text{OH}$ <sup>51</sup>	$\Delta G/\Delta G^\ddagger$ of primary attack	Regioselectivity/branching ratio: H-abstraction, $\cdot\text{OH}$ addition
Carbamazepine + HOCl <sup>52</sup>	$\Delta G/\Delta G^\ddagger$	Elucidation of mechanisms leading to experimentally observed products

423

424

425

426 Table 7: Illustrative examples of estimated thermodynamic data

System	Calculation types(s)	Gained information
HOCl/HOBr <sup>22</sup>	$\Delta G$	Estimates of unknown equilibria between

		HOX/XOX/X <sub>2</sub> (X=Cl,Br)
Halamines <sup>53</sup>	$\Delta G$ /LFER	Estimated pK <sub>a</sub> of chlor-/bromamines
Phenols <sup>38</sup>	$\Delta G$ /LFER	Estimated pK <sub>a</sub> of phenols
Sulfonamides <sup>23</sup>	$\Delta G$ /LFER	Estimated $\Delta G^\circ$ (redox potential)

427

## 428 PRACTICAL IMPLICATIONS AND OUTLOOK

### 429 *Reaction kinetics*

430 The abatement of organic micropollutants by oxidation processes is governed by  
 431 reaction kinetics. Second-order rate constants for oxidation reactions can be  
 432 determined experimentally or estimated by conventional QSAR methods. Both  
 433 approaches have limitations. Alternatively, QSAR-based approaches with QC  
 434 descriptors or *ab initio* estimations can be applied. QSAR-type approaches provide  
 435 typically reasonable results for second-order rate constants within a factor of 2-4 from  
 436 measured values. This is similar to differences between experimental studies. *ab initio*  
 437 calculations of  $k$  have shown some success for  $\cdot\text{OH}$  and other radicals. The  
 438 application to other oxidants is largely unexplored, deserving systematic studies, and  
 439 the reasons for the poor agreement with experiments need to be elucidated.

440 QSAR models with QC descriptors have been developed for the estimation of rate  
 441 constants for ozone and hydroxyl radical. For chlorine, chlorine dioxide, and ferrate  
 442 (VI), QSAR models using Hammett or Taft constants were successfully developed.<sup>6</sup>  
 443 Therefore, molecular descriptors representative of a substituent effect may manifest a  
 444 close correlation with rate constants, similar to  $E_{\text{HOMO}}$  or  $E_{\text{NBO}}$  for ozone.<sup>3</sup> A  
 445 concurrent use of other QC descriptors such as bond dissociation energies could lead  
 446 to multivariate models that surpass current QC-based QSARs.

### 447 *Formation of transformation products*

448 Prediction of transformation products formed from micropollutants during oxidative  
 449 water treatment is still a challenge. *ab initio* predictions are currently not possible, but  
 450 QC computations can assist predictions of transformation products on several levels:  
 451 (i) Confirmation of postulated reaction products by Gibbs free energy calculations,  
 452 (ii) assessment of the feasibility of postulated transient products, which are not  
 453 accessible experimentally, (iii) evaluation of reaction pathways with multiple reaction  
 454 channels, (iv) calculation of regioselectivity and (v) calculation of physical chemical  
 455 properties (e.g., pK<sub>a</sub>, standard reduction potentials).

456 In a recently developed pathway prediction system, reactions of organic moieties with  
457 ozone from experimental studies were compiled and integrated into a software using a  
458 chemoinformatics tool, applying reaction rules to predict transformation products.  
459 This *in silico* prediction system also includes an option for prediction of second-order  
460 reaction rate constants based on QSAR-type correlations of second-order rate  
461 constants with molecular orbital energies of target substances.<sup>13</sup> However, on-the-fly  
462 theoretical thermodynamic computations for different reaction channels remain to be  
463 implemented. They are currently limited due to the lack of a reliable and affordable  
464 model chemistry/software for target substances, oxidants, intermediates, and products.

#### 465 *Outlook*

466 Testing the thermodynamic feasibility of a proposed reaction mechanism based on  
467  $\Delta G_{\text{rxn}}$  is relatively easy, and should become a standard approach whenever a  
468 mechanism is proposed based on experimental results. In such analyses we need to  
469 consider that intermediate steps can be endergonic, and that kinetic control of the  
470 reaction may lead to the thermodynamically less favorable products.

471 Detailed mechanistic studies, including the calculation of  $\Delta G^\ddagger$ , have been mostly  
472 limited to hydroxyl radical, for which the chemistry is the most well-understood to  
473 date. With further experimental mechanistic studies, it should be possible to gain a  
474 better understanding of the reactivity of other oxidants reacting by addition or atom  
475 transfer (e.g., HOCl/HOBr/Cl<sub>2</sub>O/O<sub>3</sub>). Moreover, theoretically proposed mechanisms  
476 with  $\Delta G^\ddagger$  can be further verified provided that experimental  $\Delta G^\ddagger$  for the corresponding  
477 reaction channel can be obtained from the temperature dependence of the reaction rate  
478 (i.e., from the Arrhenius equation). Eventually, such mechanistic insight based on a  
479 combined experimental and computational approach could lead to pathway prediction  
480 systems that cover oxidants beyond O<sub>3</sub>.

#### 481 SUPPORTING INFORMATION

482 Computational details; further reading on calibration of QC methods, implicit and  
483 explicit solvation models, influence of the model chemistry on mechanistic  
484 calculations, speciation in reaction kinetics, rate expressions for oxidation reactions,  
485 regioselectivity and (de-)localization of molecular orbitals, the reaction coordinate of  
486 electron transfer reactions, multireference character and singlet diradicals; 4 Figures,  
487 1 Table.

488

#### 489 BIOGRAPHICAL INFORMATION

490  
491 **Peter R. Tentscher** received a PhD in chemistry from EPFL, The Swiss Federal  
492 Institute of Technology, Lausanne, followed by post-doctoral stays at EPFL and  
493 Eawag. He is currently a visiting scientist at Aalborg University. His research  
494 interests are in computational chemistry and aqueous oxidation chemistry.

495 **Minju Lee** received a PhD in environmental chemistry from EPFL and is currently a  
496 postdoctoral fellow at the University of Washington supported by the Swiss National  
497 Science Foundation Early Postdoc.Mobility fellowship, investigating the application  
498 of 3D-printed microfluidics for chemistry of oxidation processes.

499 **Urs von Gunten** received a PhD in Chemistry from the ETH, the Swiss Federal  
500 Institute of Technology in Zurich and is currently a full professor at EPFL and a  
501 senior researcher at Eawag, the Swiss Federal Institute of Aquatic Science and  
502 Technology. His main interests are kinetic and mechanistic studies of disinfection and  
503 abatement of micropollutants during oxidative processes.

504

## 505 REFERENCES

506

507

- 508 1. von Gunten, U., Oxidation Processes in Water Treatment: Are We on  
509 Track? *Environmental Science & Technology* **2018**, *52*, 5062-5075.
- 510 2. NDRL/NIST Solution Kinetics Database on the Web.  
511 <http://kinetics.nist.gov/solution/>.
- 512 3. von Sonntag, C.; von Gunten, U., *Chemistry of ozone in water and*  
513 *wastewater treatment. From basic principles to applications*. IWA: London, 2012.
- 514 4. Deborde, M.; von Gunten, U., Reactions of chlorine with inorganic and  
515 organic compounds during water treatment - Kinetics and mechanisms: A critical  
516 review. *Water Research* **2008**, *42*, 13-51.
- 517 5. Heeb, M. B.; Criquet, J.; Zimmermann-Steffens, S. G.; von Gunten, U.,  
518 Oxidative treatment of bromide-containing waters: Formation of bromine and its  
519 reactions with inorganic and organic compounds — A critical review. *Water*  
520 *Research* **2014**, *48*, 15-42.
- 521 6. Hoigné, J.; Bader, H., Kinetics of reactions of chlorine dioxide (OCLO) in  
522 water - I. Rate constants for inorganic and organic compounds. *Wat. Res.* **1994**,  
523 *28*, 45-55.
- 524 7. Sharma, V. K.; Zboril, R.; Varma, R. S., Ferrates: Greener Oxidants with  
525 Multimodal Action in Water Treatment Technologies. *Accounts of Chemical*  
526 *Research* **2015**, *48*, 182-191.
- 527 8. Waldemer, R. H.; Tratnyek, P. G., Kinetics of Contaminant Degradation by  
528 Permanganate. *Environmental Science & Technology* **2006**, *40*, 1055-1061.
- 529 9. Guan, X. H.; He, D.; Ma, J.; Chen, G. H., Application of permanganate in the  
530 oxidation of micropollutants: a mini review. *Frontiers of Environmental Science &*  
531 *Engineering in China* **2010**, *4*, 405-413.

- 532 10. Lee, Y.; von Gunten, U., Quantitative structure-Activity relationships  
533 (QSARs) for the transformation of organic micropollutants during oxidative  
534 water treatment. *Water Research* **2012**, *46*, 6177-6195.
- 535 11. Minakata, D.; Li, K.; Westerhoff, P.; Crittenden, J., Development of a Group  
536 Contribution Method To Predict Aqueous Phase Hydroxyl Radical (HO center  
537 dot) Reaction Rate Constants. *Environmental Science & Technology* **2009**, *43*,  
538 6220-6227.
- 539 12. Lee, M.; Zimmermann-Steffens, S. G.; Arey, J. S.; Fenner, K.; von Gunten, U.,  
540 Development of Prediction Models for the Reactivity of Organic Compounds with  
541 Ozone in Aqueous Solution by Quantum Chemical Calculations: The Role of  
542 Delocalized and Localized Molecular Orbitals. *Environmental Science &*  
543 *Technology* **2015**, *49*, 9925-9935.
- 544 13. Lee, M.; Blum, L. C.; Schmid, E.; Fenner, K.; von Gunten, U., A computer-  
545 based prediction platform for the reaction of ozone with organic compounds in  
546 aqueous solution: kinetics and mechanisms. *Environmental Science: Processes &*  
547 *Impacts* **2017**, *19*, 465-476.
- 548 14. Guo, X.; Minakata, D.; Niu, J.; Crittenden, J., Computer-Based First-  
549 Principles Kinetic Modeling of Degradation Pathways and Byproduct Fates in  
550 Aqueous-Phase Advanced Oxidation Processes. *Environmental Science &*  
551 *Technology* **2014**, *48*, 5718-5725.
- 552 15. Pari, S.; Wang, I. A.; Liu, H.; Wong, B. M., Sulfate radical oxidation of  
553 aromatic contaminants: a detailed assessment of density functional theory and  
554 high-level quantum chemical methods. *Environmental Science: Processes &*  
555 *Impacts* **2017**, *19*, 395-404.
- 556 16. Yu, H.; Chen, J.; Xie, H.; Ge, P.; Kong, Q.; Luo, Y., Ferrate(vi) initiated  
557 oxidative degradation mechanisms clarified by DFT calculations: a case for  
558 sulfamethoxazole. *Environmental Science: Processes & Impacts* **2017**, *19*, 370-  
559 378.
- 560 17. Cramer, C. J., *Essentials of Computational Chemistry*. John Wiley&Sons:  
561 Chichester, England, 2004.
- 562 18. Trogolo, D.; Arey, J. S., Equilibria and Speciation of Chloramines,  
563 Bromamines, and Bromochloramines in Water. *Environmental Science &*  
564 *Technology* **2017**, *51*, 128-140.
- 565 19. Helgaker, T.; Jorgensen, P.; Olsen, J., *Molecular electronic-structure theory*.  
566 John Wiley&Sons: Chichester, England, 2000.
- 567 20. Karton, A., Post-CCSD(T) contributions to total atomization energies in  
568 multireference systems. *The Journal of Chemical Physics* **2018**, *149*, 034102.
- 569 21. Trogolo, D.; Arey, J. S.; Tentscher, P. R., Gas phase ozone reactions with a  
570 structurally diverse set of molecules: barrier heights and reaction energies  
571 evaluated by coupled cluster and density functional calculations. *J Phys Chem A*  
572 *submitted*. **2018**.
- 573 22. Sivey, J. D.; Arey, J. S.; Tentscher, P. R.; Roberts, A. L., Reactivity of BrCl,  
574 Br<sub>2</sub>, BrOCl, Br<sub>2</sub>O, and HOBr Toward Dimethenamid in Solutions of Bromide +  
575 Aqueous Free Chlorine. *Environmental Science & Technology* **2013**, *47*, 1330-  
576 1338.
- 577 23. Tentscher, P. R.; Eustis, S. N.; McNeill, K.; Arey, J. S., Aqueous Oxidation of  
578 Sulfonamide Antibiotics: Aromatic Nucleophilic Substitution of an Aniline  
579 Radical Cation. *Chemistry – A European Journal* **2013**, *19*, 11216-11223.

- 580 24. Goerigk, L.; Hansen, A.; Bauer, C.; Ehrlich, S.; Najibi, A.; Grimme, S., A look  
581 at the density functional theory zoo with the advanced GMTKN55 database for  
582 general main group thermochemistry, kinetics and noncovalent interactions.  
583 *Physical Chemistry Chemical Physics* **2017**, *19*, 32184-32215.
- 584 25. Marenich, A. V.; Cramer, C. J.; Truhlar, D. G., Universal Solvation Model  
585 Based on Solute Electron Density and on a Continuum Model of the Solvent  
586 Defined by the Bulk Dielectric Constant and Atomic Surface Tensions. *The Journal*  
587 *of Physical Chemistry B* **2009**, *113*, 6378-6396.
- 588 26. Thapa, B.; Schlegel, H. B., Improved pKa Prediction of Substituted  
589 Alcohols, Phenols, and Hydroperoxides in Aqueous Medium Using Density  
590 Functional Theory and a Cluster-Continuum Solvation Model. *The Journal of*  
591 *Physical Chemistry A* **2017**, *121*, 4698-4706.
- 592 27. Tentscher, P. R.; Seidel, R.; Winter, B.; Guerard, J. J.; Arey, J. S., Exploring  
593 the Aqueous Vertical Ionization of Organic Molecules by Molecular Simulation  
594 and Liquid Microjet Photoelectron Spectroscopy. *The Journal of Physical*  
595 *Chemistry B* **2015**, *119*, 238-256.
- 596 28. McKechnie, S.; Booth, G. H.; Cohen, A. J.; Cole, J. M., On the accuracy of  
597 density functional theory and wave function methods for calculating vertical  
598 ionization energies. *The Journal of Chemical Physics* **2015**, *142*, 194114.
- 599 29. Guerard, J. J.; Arey, J. S., Critical Evaluation of Implicit Solvent Models for  
600 Predicting Aqueous Oxidation Potentials of Neutral Organic Compounds. *Journal*  
601 *of Chemical Theory and Computation* **2013**, *9*, 5046-5058.
- 602 30. Guerard, J. J.; Tentscher, P. R.; Seijo, M.; Samuel Arey, J., Explicit solvent  
603 simulations of the aqueous oxidation potential and reorganization energy for  
604 neutral molecules: gas phase, linear solvent response, and non-linear response  
605 contributions. *Physical Chemistry Chemical Physics* **2015**, *17*, 14811-14826.
- 606 31. Galano, A.; Alvarez-Idaboy, J. R., A computational methodology for  
607 accurate predictions of rate constants in solution: Application to the assessment  
608 of primary antioxidant activity. *Journal of Computational Chemistry* **2013**, *34*,  
609 2430-2445.
- 610 32. Baerends, E. J.; Gritsenko, O. V.; van Meer, R., The Kohn–Sham gap, the  
611 fundamental gap and the optical gap: the physical meaning of occupied and  
612 virtual Kohn–Sham orbital energies. *Physical Chemistry Chemical Physics* **2013**,  
613 *15*, 16408-16425.
- 614 33. Tsuneda, T.; Song, J.-W.; Suzuki, S.; Hirao, K., On Koopmans' theorem in  
615 density functional theory. *The Journal of Chemical Physics* **2010**, *133*, 174101.
- 616 34. Zhang, H.-Y.; Sun, Y.-M.; Zhang, G.-Q.; Chen, D.-Z., Why Static Molecular  
617 Parameters Cannot Characterize the Free Radical Scavenging Activity of Phenolic  
618 Antioxidants. *Quantitative Structure-Activity Relationships* **2000**, *19*, 375-379.
- 619 35. Glendening, E. D.; Landis, C. R.; Weinhold, F., Natural bond orbital  
620 methods. *Wiley Interdisciplinary Reviews: Computational Molecular Science* **2011**,  
621 *2*, 1-42.
- 622 36. Brown, J. J.; Cockroft, S. L., Aromatic reactivity revealed: beyond  
623 resonance theory and frontier orbitals. *Chemical Science* **2013**, *4*, 1772-1780.
- 624 37. Naumov, S.; von Sonntag, C., Quantum Chemical Studies on the Formation  
625 of Ozone Adducts to Aromatic Compounds in Aqueous Solution. *Ozone: Science &*  
626 *Engineering* **2010**, *32*, 61-65.
- 627 38. Tentscher, P. R.; Bourgin, M.; von Gunten, U., Ozonation of Para-  
628 Substituted Phenolic Compounds Yields p-Benzoquinones, Other Cyclic  $\alpha,\beta$ -

629 Unsaturated Ketones, and Substituted Catechols. *Environmental Science &*  
630 *Technology* **2018**, *52*, 4763-4773.

631 39. Nolte, T. M.; Peijnenburg, W. J. G. M., Use of quantum-chemical descriptors  
632 to analyze reaction rate constants between organic chemicals and  
633 superoxide/hydroperoxyl ( $O_2^{\cdot-}/HO_2^{\cdot}$ ). *Free Radical Research* **2018**, 1-411.

634 40. Luo, X.; Yang, X.; Qiao, X.; Wang, Y.; Chen, J.; Wei, X.; Peijnenburg, W. J. G.  
635 M., Development of a QSAR model for predicting aqueous reaction rate constants  
636 of organic chemicals with hydroxyl radicals. *Environmental Science: Processes &*  
637 *Impacts* **2017**, *19*, 350-356.

638 41. Minakata, D.; Crittenden, J., Linear Free Energy Relationships between  
639 Aqueous phase Hydroxyl Radical Reaction Rate Constants and Free Energy of  
640 Activation. *Environmental Science & Technology* **2011**, *45*, 3479-3486.

641 42. Minakata, D.; Mezyk, S. P.; Jones, J. W.; Daws, B. R.; Crittenden, J. C.,  
642 Development of Linear Free Energy Relationships for Aqueous Phase Radical-  
643 Involved Chemical Reactions. *Environmental Science & Technology* **2014**, *48*,  
644 13925-13932.

645 43. Nolte, T. M.; Peijnenburg, W. J. G. M., Aqueous-phase photooxygenation of  
646 enes, amines, sulfides and polycyclic aromatics by singlet ( $a^1\Delta_g$ ) oxygen:  
647 prediction of rate constants using orbital energies, substituent factors and  
648 quantitative structure–property relationships. *Environmental Chemistry* **2017**,  
649 *14*, 442-450.

650 44. Arnold, W. A.; Oueis, Y.; O'Connor, M.; Rinaman, J. E.; Taggart, M. G.;  
651 McCarthy, R. E.; Foster, K. A.; Latch, D. E., QSARs for phenols and phenolates:  
652 oxidation potential as a predictor of reaction rate constants with  
653 photochemically produced oxidants. *Environmental Science: Processes & Impacts*  
654 **2017**, *19*, 324-338.

655 45. Arnold, W. A., One electron oxidation potential as a predictor of rate  
656 constants of N-containing compounds with carbonate radical and triplet excited  
657 state organic matter. *Environmental Science: Processes & Impacts* **2014**, *16*, 832-  
658 838.

659 46. Minakata, D.; Kamath, D.; Maetzold, S., Mechanistic Insight into the  
660 Reactivity of Chlorine-Derived Radicals in the Aqueous-Phase UV–Chlorine  
661 Advanced Oxidation Process: Quantum Mechanical Calculations. *Environmental*  
662 *Science & Technology* **2017**, *51*, 6918-6926.

663 47. Trogolo, D.; Mishra, B. K.; Heeb, M. B.; von Gunten, U.; Arey, J. S., Molecular  
664 Mechanism of NDMA Formation from N,N-Dimethylsulfamide During Ozonation:  
665 Quantum Chemical Insights into a Bromide-Catalyzed Pathway. *Environmental*  
666 *Science & Technology* **2015**, *49*, 4163-4175.

667 48. Kamath, D.; Mezyk, S. P.; Minakata, D., Elucidating the Elementary  
668 Reaction Pathways and Kinetics of Hydroxyl Radical-Induced Acetone  
669 Degradation in Aqueous Phase Advanced Oxidation Processes. *Environmental*  
670 *Science & Technology* **2018**, *52*, 7763-7774.

671 49. Liu, Y. D.; Selbes, M.; Zeng, C.; Zhong, R.; Karanfil, T., Formation  
672 Mechanism of NDMA from Ranitidine, Trimethylamine, and Other Tertiary  
673 Amines during Chloramination: A Computational Study. *Environmental Science &*  
674 *Technology* **2014**, *48*, 8653-8663.

675 50. Spahr, S.; Cirpka, O. A.; von Gunten, U.; Hofstetter, T. B., Formation of N-  
676 Nitrosodimethylamine during Chloramination of Secondary and Tertiary

677 Amines: Role of Molecular Oxygen and Radical Intermediates. *Environmental*  
678 *Science & Technology* **2017**, *51*, 280-290.

679 51. Xiao, R.; Noerpel, M.; Ling Luk, H.; Wei, Z.; Spinney, R., Thermodynamic  
680 and kinetic study of ibuprofen with hydroxyl radical: A density functional theory  
681 approach. *International Journal of Quantum Chemistry* **2013**, *114*, 74-83.

682 52. Tandarić, T.; Vrček, V.; Šakić, D., A quantum chemical study of HOCl-  
683 induced transformations of carbamazepine. *Organic & Biomolecular Chemistry*  
684 **2016**, *14*, 10866-10874.

685 53. Heeb, M. B.; Kristiana, I.; Trogolo, D.; Arey, J. S.; von Gunten, U., Formation  
686 and reactivity of inorganic and organic chloramines and bromamines during  
687 oxidative water treatment. *Water Research* **2017**, *110*, 91-101.

688

689